MULTI-RESOLUTION DUAL CONTOURING FROM VOLUMETRIC DATA

Ricardo Uribe Lobello, Florent Dupont and Florence Denis
Université de Lyon, CNRS, LIRIS, UMR5205, F-69622, Villeurbanne, France

Keywords: Surface Modeling, Image-based Modeling, Multi-resolution Modeling.

Abstract: We present a Multi-Resolution Dual method based on an incremental octree-based refinement strategy. Our solution is able to generate multi-resolution surfaces from segmented volumetric data. It extends the Dual Marching Cubes algorithm over a generalized octree and guarantees that the produced surfaces are always manifold by introducing a new cell-based criterion for dual vertices generation. Moreover, we propose a top-bottom refinement algorithm that is able to locally adapt the mesh resolution according to a curvature parameter. Our algorithm is suitable to process volumetric data sets and we show on different volumes that the produced surfaces are manifold and approximate well the original object.

1 INTRODUCTION

Volumetric data is a very common source of information in several domains. However, processing it directly can be expensive. This has boosted the development of surface extraction methods as a more efficient and compact representation. In recent years, the size of available data sets has steadily increased. As consequence, many multi-resolution algorithms have been proposed in order to extract adaptive surfaces. Furthermore, if the surface must be usable in post-processing applications such as numerical simulations, it must be a closed manifold and fulfill some quality criteria.

2 RELATED WORK

There is a vast bibliography concerning surface generation methods from segmented volumetric data. The Marching Cubes (MC) algorithm (Lorensen and Cline, 1987) is based on a regular division of the volumetric data in cubical cells that can be processed separately. All possible intersection patterns have been reduced to 14 cases pre-calculated in a look-up table. However, MC generates very dense surfaces and many degenerated triangles.

Several algorithms have been proposed in order to overcome MC limitations (Wilhelms and Van Gelder, 1992). Kobbelt *et al.* (Kobbelt et al., 2001) replace the regular grid by an octree and process only the cells intersecting the surface. Varadhan *et al.* (Varadhan et al., 2004) control the octree subdivision using a topology preserving criterion in order to make every cell MC-compatible and obtain consistent multi-resolution meshes. (Kazhdan et al., 2007) have proposed an algorithm to extract closed manifold surfaces with MC on unrestricted octrees. However, as surface vertices remain located on the edges of octree cells, this algorithm reduces to MC inside cells and sharp features can be lost during reconstruction.

Dual contouring (DC) methods (Ju et al., 2002) are able to generate multi-resolution meshes and to reproduce sharp features in the presence of Hermite Data. In these methods, surface vertices are not created on cell's edges but one vertex is generated inside every cell. However, this approach can make arise topological problems and non-manifold configurations.

By limiting DC octree adaptivity, Varadhan *et al.* (Varadhan et al., 2003) have proposed an improved DC that avoids non-manifold configurations. Then, in Dual Marching Cubes (DMC), Nielson (Nielson, 2004) uses a look-up table to generate surfaces that are dual to those generated by Marching cubes by allowing cells to contain more than one dual vertex so to solve the non-manifold vertex configurations.

However, we have verified that by simply applying the DMC algorithm, non-manifold edge configurations can still appear where cases 17 and 20 of the look-up table of DMC share a common ambiguous face (see figure 1).

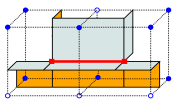

Figure 1: Left non-manifold edge configuration (line in red).

In order to solve these problems, several approaches propose to create dual grids extracted from an octree data structure. These grids are aligned to features of the surface by using Hermite data on the octree cells. Then, the isosurface is extracted by contouring these dual grids using Marching cubes (Schaefer and Warren, 2005) or Marching Tetrahedra (Manson and Schaefer, 2010). However, dual grid approaches can generate self-intersected surfaces or many degenerate triangles.

Finally, Manifold Dual Contouring (MDC) (Schaefer et al., 2007) uses DMC over a regular octree and a topology preserving criterion in order to produce adaptive manifold meshes that maintain the topology of the original object. Nevertheless, it uses a bottom-up strategy that is not suitable to handle large data sets.

2.1 Contributions

In order to extract efficiently closed manifold surfaces from a regular grid, we consider that a dual approach will be the most suitable. Therefore, we have decided to use a DMC based algorithm. Our main contributions to this method are: 1) The use of a generalized hashed octree as base for a multi-resolution surface generation algorithm. 2) The presentation of a simple octree cell based algorithm to detect and solves non-manifold configurations arising in DMC. 3) A top-bottom octree-based refinement algorithm that is able to generate multi-resolution compact manifolds based on the surface normals information.

3 MULTI-RESOLUTION DUAL MARCHING CUBES WITH MANIFOLD PRESERVATION

From now, let be $\{F(x)|\Re^3 \longrightarrow \Re\}$ the indicator function so that $\{F(x) = 1\}$ if x is inside the segmented object and zero otherwise. We start by defining some preliminary concepts and notation.

3.1 Preliminaries and Notation

In this paper, *cell volume* will indicate the interior volume of a cell.

Definition 1. *A cell c is a graph $c = \{V,E\}$ defined by eight vertices $V = \{v_0, v_1, ..., v_7\}$ and twelve edges $E = \{e_0, e_1, ..., e_{11}\}$ with the connectivity of a cube.*

A cell vertex is labelled as *solid* if it is inside the volume and *empty* otherwise. The set of solid vertices in a cell c is denoted by $S(c)$ and the set of empty vertices $E(c)$. $|S(c)|$ and $|E(c)|$ denote the cardinality of each set respectively.

Definition 2. *A* solid-edge *(resp.* empty-edge*) is an edge whose two endpoints are solid (resp. empty). Edges that have a solid endpoint and an empty one are defined as* intersection-edges *(Wang and Chen, 2008). A face is* solid *(resp.* empty*) if all its vertices are solid (resp.* empty*), otherwise, it is an* intersected-face.

Definition 3. *An* ambiguous face *exists when the face contains two interleaved solid vertices.*

As in (Wang and Chen, 2008), we have decided to use the connected components with respect to the solid and empty vertices to determine the dual vertices that have to be created inside a cell. We define a connected component as follows:

Definition 4. *A* connected component *inside a cell c is a sub-graph where all two solid (resp. empty) vertices are connected by a path of solid-edges (resp. empty-edges) noted as $\phi(c)_s$ (resp. $\phi(c)_e$). The number of connected components are called $|\phi(c)_s|$ and $|\phi(c)_e|$ respectively (Wang and Chen, 2008).*

Finally, the set of dual vertices inside a cell c is defined as $D(c) = \{d_0, d_1 ...\}$ and the number of dual vertices as $|D(c)|$.

3.2 Dual Vertex Creation with Manifold Preservation

We propose an algorithm that generates directly a closed manifold by using the solid/empty connected components of the cell vertices. Contrary to Wang and Chen, no post-processing step is necessary to repair non-manifold edges and ensure that the produced surface is topologically correct. Our dual vertices generation algorithm is based on the following rules:

Rule 1. *Let c be a cell. dual vertices are only created in cells where $0 < |S(c)| < 8$.*

Rule 2. *Let c be a cell. If $|S(c)| < 5$ then $|D(c)| = |\phi(c)_s|$ and if $|S(c)| >= 5$ then $|D(c)| = |\phi(c)_e|$.*

A cell is homogeneous if all its corners are either inside or outside of $F(x)$:

Rule 3. *Let c be a non homogeneous cell, every dual vertex $d_i \in D(c)$ generated from a solid connected component $\phi(c)_s$ (resp. empty connected component*

$\phi(c)_e$) is associated with the set of intersection-edges that leaves $\phi(c)_s$ (resp. $\phi(c)_e$).

The simple application of the three precedent rules produces the same patch configuration of Dual Marching Cubes (Nielson, 2004). This patches will generate non-manifold edges when two cells with cases 17 and 20 share an ambiguous face. To fix this, we propose to look at the two cells and choose the right (solid/empty) components configuration to generate the dual vertices. Problematic cases are essentially those where neighbouring cells have between 5 and 6 vertices and they share an ambiguous face. Next rule allows us to deal with the cases that generate non-manifold configurations in DMC.

Rule 4. *Let be c a cell. c can have been marked with a component(solid/empty):*

- *if c is marked, generate dual vertices with the indicated component.*
- *Otherwise, use rules 1 to 3 to determine the component (solid or empty) to be used to generate the dual vertices in c. Then, if c has ambiguous faces, mark every adjacent cell through an ambiguous face with the component that has been used for c.*

Previous rule spreads the topological choice that has been done in a cell through all its ambiguous faces and ensures the manifold correctness of the generated surface. A cell with $|S(c)| = 6$ can only have one ambiguous face, so, the possible patches generated with this cell are illustrated in figure 2.

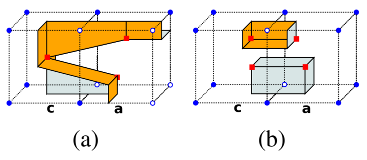

Figure 2: Possible patches for two 6 solid vertices cells connected by an ambiguous face. (a) solid component, (b) empty component. Dual vertices are noted as red squares.

A cell with $|S(c)| = 5$ can have zero, one or three ambiguous faces, the possible patches extracted with our rules are illustrated in figure 3. The previous criterion depends only on the connected components of two neighbouring cells. As its application is local, we have designed exhaustive tests which confirm that, with our criterion, all non-manifold configurations arising in DMC are correctly handled.

3.3 Octree Construction

As multi-resolution data structure, we have implemented a linear octree that uses a Morton Code (Lewiner et al., 2010). This code is a compact integer

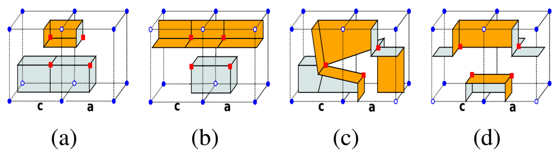

Figure 3: Pairs of cells sharing a common ambiguous face. (a) and (b) Empty Connectivity, (c) and (d) Solid connectivity. Dual vertices are noted as red squares.

representation that allows us to encode hierarchical relationships between octree cells together with geometrical information about their position in the domain. Furthermore, a simple array can be used to store octree cells in order to improve access times. As our octree is generalized, we need to store initial and final cell coordinates in ever octree cell, together with cell corner's values and the collapsed flag.

Our octree construction algorithm is an iterative top-bottom algorithm that builds an octree until a specified level of resolution. Octree cells are initially divided if they are inhomogeneous and if it is not complex as defined below.

Definition 5. *Let C be a cell. C is* complex *if at least one of its faces is complex. A cell face is complex if:*

- *It intersects $F(x)$ and all its vertices are either inside or outside $F(x)$.*
- *At least one of its edges intersects $F(x)$ more than once.*

Complex cell criterion allows us to detect cells that contain a piece of the surface that is smaller than the current level of subdivision. This strategy allows us to just check voxels that belongs to cell's faces to assure that all cells intersected by $F(x)$ are going to be processed.

Rule 5. Subdivision Rule: *If a cell C is inhomogeneous or is complex, it has to be subdivided. Otherwise, it is marked as an octree leaf.*

The application of the subdivision rule will generate an octree where all leaves cells that intersect $F(x)$ are at the same level. Then, our dual vertex generation rules (precedent section) can be applied in every cell (ou pair of cells) to produce compact regular meshes.

3.4 Multi-resolution Meshes

In order to generate multi-resolution surfaces adapted to the curvature of $F(x)$. We propose to use a criterion based on the normals at the intersection points of cell edges with $F(x)$. We have used a surface approach based on the measure of the average of unitary normals in the neighbourhood of the edge intersection with $F(x)$ (Flin, 2005).

Criterion 1. *Let C be a cell and $I_{i=0...n}$ its intersection points with $F(x)$. Let be $n_{i=0...n}$ the normals on $I_{i=0...n}$. If Max($n_i \bullet n_j | i \neq j\}$) > δ, C must be subdivided. δ is a user provided parameter with values in the closed interval* $[0,1]$.

The previous criterion gives valuable information about the shape of $F(x)$ inside the cell. As consequence, a $\delta \to 0$ will produce an almost regular mesh. On the contrary, $\delta \to 1$ will generate a highly simplified surface. This can lead to lose sharp features in the generated surface. Cells that have not been subdivided until the maximal octree depth are marked as *collapsed*. The octree creation method is implemented iteratively and it is described in algorithm 1.

Algorithm 1: Build Octree algorithm.

```
input  : Root cell of the octree $c$. Minimal level of the octree
         $minLevel$ and maximal subdivision level $maxLevel$.
output: Octree regular until level $minLevel$ and adaptive between
         $minLevel$ and $maxLevel$.
Add cell c to toProcess list;
while toProcess is not empty do
    currentCell ← GetFirstElement (toProcess) ;
    if GetLevel (minLevel >= GetLevel (currentCell) And
    currentCell) < maxLevel then
        if isNotComplex(currentCell) then
            if isNotPlanar(currentCell) then
                Subdivide:
                Comment: currentCell must be subdivided;
                $S = \{q_1, ..., q_8\}$ ← Divide (currentCell) ;
                foreach cell $q_i$ in S do
                    Adds $q_i$ to the toProcess list
                end
            else Mark currentCell as a leaf and as collapsed
        else Goto Subdivide
    else Goto Subdivide
end
```

A *collapsed* cell can generate topological problems if it is adjacent to cells of higher resolution. This is because at some resolution levels, the shape of $F(x)$ can traverse several times edges or faces of a collapsed cell (see figure 4a) generating non manifold configuration in the final surface.

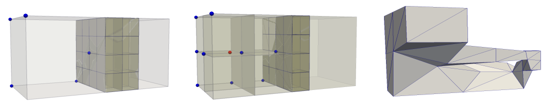

Figure 4: Two neighbours cells are illustrated, blue spheres are cells corners inside $F(x)$. Collapsed cell (left) is in clair, deeper cells are in dark. (a) Our algorithm detects a complex face and subdivides the left cell (b), (c) The tunnel between cells is captured and a manifold surface is generated.

In order to solve this, we proceed as follows, for each cell q marked as collapsed, we obtain its face adjacent cells at the same level (see figure 4a in clear). Then, for each adjacent cell, we extract the set of leaf cells A_i that are face adjacent to q. For each cell $c \in A_i$, we detect the face $f \in c$ adjacent to q and we extract the values of $F(x)$ at its vertices. Doing it for all cells in A_i allows us to build a projection of $F(x)$ over q's face as an image. Then, if any one of these face images are complex, a non manifold configuration will be generated between these cells. Once the complex topology has been detected, we decided to subdivide q until complex faces are eliminated and the subdivision is good enough to capture the topology of $F(x)$ (see figure 4b and c).

However, other topological problems can be generated by q's subdivision, so our algorithm recursively checks if other cells have been affected and extends the validation area. Our algorithm stops when no cell presents complex faces. The resume of the method can be seen in the algorithm 2.

Algorithm 2: Local refinement algorithm.

```
input  : Set $T$ of collapsed cells $c$. A level of refinement $l$.
output: Set $A$ as the set of affected cells where $T \subset A$.
foreach cell $c \in T$ do  Add cell $c$ to $A$ ;
foreach cell $c \in A$ do
    Apply BuildOctree method to $c$ until level $l$;
    for faceCounter ← 1 to 6 do
        face ← GetCellFace (faceCounter);
        if face is complex then
            newAffectedCell ← GetAdjacentCell
            (c,face);
            Adds newAffectedCell to $A$ ;
        end
    end
end
```

Algorithm 2 is executed recursively and its complexity is linear over cells affected by any induced subdivision. Its execution time strongly relies on the topological complexity of $F(x)$ but our experiments have shown that no excessive subdivision is needed to fix most topological problems. In our implementation, algorithm 2 is executed after the octree construction showed in algorithm 1.

3.5 Connectivity Generation

The connectivity generation process connects the dual vertices by using a linear complexity algorithm, proposed by (Ju et al., 2002), that traverses the octree and connects the dual vertices of cells that share an intersection-edge. The dual vertices are connected by using the Rule 3 of our dual vertices generation algorithm.

3.6 Dual Vertices Localization

We propose a dual vertex localization algorithm based on the barycentre b_s of every connected component of $F(x)$ inside a cell. Let be C a leaf cell in the octree where $F(x) \cap C \neq \emptyset$. As we know the dimensions of C and its mass M, we can obtain its barycentre b_c. Then, we calculate the barycentre of $F(x) \cap C$ named b_s and its mass m_s. Finally, the mass and barycentre of the complementary of $(F(x) \cap C)$ can be calculated using equation $Mb_c = m_s b_s + m_e b_e$.

These three barycentre points and theirs cell's masses proportion can be used to approximate the position of the dual vertex d. Naturally, d will lie between b_s and b_e. This is illustrated in figure 5.

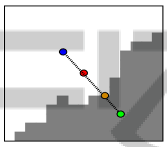

Figure 5: Cell barycentre (red), $F(x) \cap C$ barycentre (green), $(F(x) \cap C)^c$ barycentre (blue), dual vertex (yellow).

Localization methods such as Quadric Error Functions has been considered, however, QEF is not a good estimator if the surface is noisy and our experiments have shown that our method works well on smooth or noisy surfaces.

4 RESULTS AND COMPARISON

Data sets presented in this paper were generated from set of images extracted from the discretization of polygonal meshes. As quality measures, we have used the size of the mesh as number of triangles and the Hausdorff and Root-Mean-Square distances with respect to the discretized polygonal model.

4.1 Results

By applying our algorithm on multiple datasets, we have confirmed that it always generates closed manifold surfaces. An example is illustrated in figure 6 where a filigree model is generated from a 512^3 data set with $\delta = 0.05$ (curvature parameter) at 8 octree depth. Table 1 shows generation times and distance measures for the filigree model at different octree depths. Relatively long execution times in the octree construction phase of our algorithm are explained by the cost of normals calculation and complex cell criterion evaluation over discrete volumes.

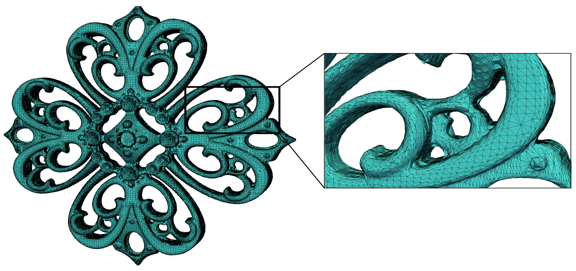

(a) Filigree surface (octree depth 8) and zoom.

Figure 6: Filigree surface extracted at three octree depths 8 from a 512^3 volumetric model.

Table 1: Filigree dataset statistics at three octree depths.

Octree Level	Depth 6	Depth 7	Depth 8
Octree Time	1.2s	3.142s	10.858s
Surface Time	2.767s	3.322s	8.099s
# Facets	15 266	66 438	255 088
RMS Dist.	0.006615	0.003103	0.001737
Hausdorff Dist.	0.024640	0.022805	0.008654

The δ parameter can be changed in order to produce simplified multi-resolution meshes. In figure 7, Wales Dragon meshes have been generated at the same octree level but with different curvature thresholds.

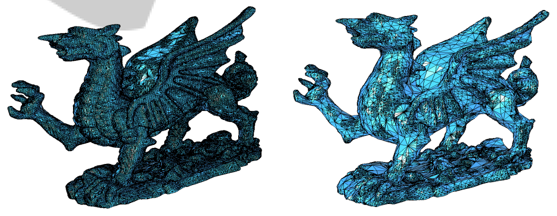

(a) Regular mesh ($\delta = 0.05$). (b) Simplified mesh ($\delta = 0.9$).

Figure 7: Wales Dragon surface generated from a volumetric data set (512^3) with a δ from 0.05 (a) to 0.9 (b), where small triangles are just necessary in highly curved regions.

Graphs in figure 8 show that the model simplification does not strongly affect the precision of our algorithm. As it can be seen, we can reduce from 180K triangles to less of 60K and geometrical error just increases from 0.009 to 0.015 approximately.

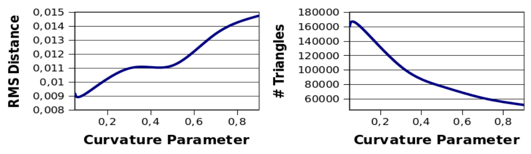

Figure 8: RMS distance and number of triangles for Wales Dragon data set with respect to the curvature parameter δ.

4.2 Comparison

In order to compare our algorithm with relevant methods, we have chosen a MC based method (Kazhdan et al., 2007) and the implementation of the dual method proposed by Schaefer and Warren (Schaefer and Warren, 2005). Results for the Dragon and Horse data sets are resumed in figure 9.

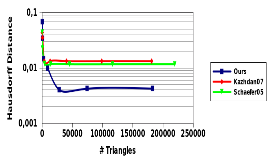

(a) Hausdorff Distance Vs #Triangles in Dragon.

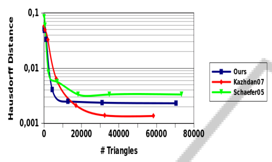

(b) Hausdorff Distance Vs #Triangles in Horse.

Figure 9: Logarithmic comparison graphs between our method (in blue), Schaefer *et al.* dual algorithm (in green) and Kazhdan *et al.* MC algorithm (in red). For similar number of triangles, our algorithm leads to smaller or same order error distances.

As it is shown in the graphs, with less triangles, our algorithm is able to obtain better or as good approximations as Kazhdan and Schaefer. This is understandable because both methods are multi-resolution extensions of MC and they restrict the surface nodes to be located on the cell's edges. surfaces produced by our algorithm are shown in figure 10.

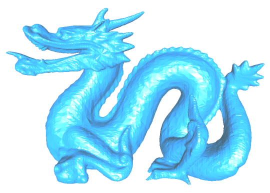

(a) Dragon.

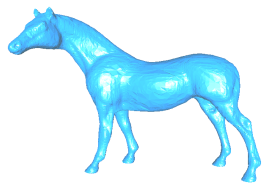

(b) Horse.

Figure 10: Dragon (182840 triangles) and Horse (70498 triangles) surfaces generated from 512^3 volumes with a 9 depth octree and a curvature parameter δ of 0.25.

5 CONCLUSIONS AND PERSPECTIVES

In this paper we have presented a algorithm based on Nielson's DMC together with an efficient octree implementation in order to generate compact and manifold multi-resolution meshes. In addition, we have proposed a dual vertex localization method based on connected components to improve surface approximation. In further work, we believe that our approach can be integrated on an Out-of-Core strategy in order to process large volumetric data sets.

ACKNOWLEDGEMENTS

This research was partially supported by the French National Project PEPS INS2I CNRS ImagEar3D. Thanks to the Stanford CGL, Georgia Tech and Cyberware for the models used in this paper.

REFERENCES

Flin, F. (2005). Adaptative estimation of normals and surface area for discrete 3d objects. *IEEE Transactions on Image Processing*, 14(5):585–596.

Ju, T., Losasso, F., Schaefer, S., and Warren, J. (2002). Dual contouring of hermite data. In *Proceedings of SIGGRAPH '02*, pages 339–346.

Kazhdan, M., Klein, A., Dalal, K., and Hoppe, H. (2007). Unconstrained isosurface extraction on arbitrary octrees. In *Proceedings of Symposium on Geometry processing*, pages 125–133.

Kobbelt, L. P., Botsch, M., Schwanecke, U., and Seidel, H.-P. (2001). Feature sensitive surface extraction from volume data. In *SIGGRAPH '01*, pages 57–66.

Lewiner, T., Mello, V., Peixoto, A., Pesco, S., and Lopes, H. (2010). Fast generation of pointerless octree duals. In *Computer Graphics Forum*, volume 29, pages 1661–1669.

Lorensen, W. and Cline, H. (1987). Marching cubes: A high resolution 3D surface construction algorithm. In *SIGGRAPH '87*, volume 87, pages 163–169.

Manson, J. and Schaefer, S. (2010). Isosurfaces over simplicial partitions of multiresolution grids. *Computer Graphics Forum*, 29(2):377–385.

Nielson, G. M. (2004). Dual marching cubes. In *Proceedings of the conference on Visualization '04*, VIS '04, pages 489–496.

Schaefer, S., Ju, T., and Warren, J. (2007). Manifold dual contouring. *IEEE Transactions on Visualization and Computer Graphics*, 13:610–619.

Schaefer, S. and Warren, J. D. (2005). Dual marching cubes: Primal contouring of dual grids. *Computer Graphics Forum*, pages 195–201.

Varadhan, G., Krishnan, S., Kim, Y., and Manocha, D. (2003). Feature-sensitive subdivision and isosurface reconstruction. In *Visualization, 2003.*, pages 99–106.

Varadhan, G., Krishnan, S., Sriram, T., and Manocha, D. (2004). Topology preserving surface extraction using adaptive subdivision. *In Symposium of Geometry Processing '04*.

Wang, C. and Chen, Y. (2008). Layered depth-normal images for complex geometries-part two: manifold-preserved adaptive contouring. *ASME IDETC/CIE Conference '08*.

Wilhelms, J. and Van Gelder, A. (1992). Octrees for faster isosurface generation. *ACM Trans. Graph.*, 11:201–227.